

Assessment of the role of axial vorticity in the formation of Particle Accumulation Structures in supercritical Marangoni and hybrid thermocapillary-rotation-driven flows

Marcello Lappa¹

1) Telespazio, Via Gianturco 31, Napoli, 80046, Italy (marlappa@unina.it)

ABSTRACT: Evidence is provided that when the so-called phenomenon of PAS occurs, extended regions exist where $\frac{1}{2}$ of the axial component of vorticity matches the angular frequency of the traveling wave produced by the instability of the Marangoni flow. Several cases are considered in which such axial component is varied by “injecting” vorticity into the system via rotation of one of its endwalls. The results show that both the resulting PAS lines and the trajectories of related solid particles undergo significant changes under the influence of imposed rotation. By analysis of such findings, a validation and a generalization/extension of the so-called “phase-locking” model are provided.

I. INTRODUCTION

One of the many characteristics of all dissipative systems (systems for which, evolution is driven by competition between a driving force and dissipation of energy) is that their phase trajectories are attracted by a geometric object called “attractor”. This means that different trajectories, arising from different points of the attractor, end on the attractor anyway.

In such a context, much attention has been devoted over recent years to the so-called Marangoni flow. Apart from possible technological applications (which are numerous and multivariate¹) the study of *pure* Marangoni convection with respect to flows of gravitational nature (which have enjoyed a larger attention in a variety of situations^{2,3}) has been aimed from an “ideological” synergetic point of view, to gaining further progress in the understanding of pattern-forming systems of different nature.

It is such a line of research which led to identify for supercritical (oscillatory) Marangoni flow two distinct attractors in the phase space, which are today known more or less universally as “pulsating” and “traveling” regimes, the former being featured by the periodic growth and decay of disturbances at fixed positions in space, the latter by the propagation of such disturbances along a preferred direction, see, e.g., Lappa² (the reader being also referred to Shevtsova et al.⁴ for additional exotic attractors due to the combined action of Marangoni and buoyancy forces).

More recent studies have shown that besides the existence of well defined attractors in the phase space, some special geometric objects seem also to exist in the “physical” space of such dissipative systems. Indeed, particular one-dimensional closed paths have been identified which tend to “capture” (as time passes) rigid particles seeded in the liquid (in general, tracers, which are injected in the liquid for visualization purposes) leading to the formation of apparently solid rotating threads (the so-called “particle accumulation structures”, generally referred to with the acronym “PAS”). This state should not be regarded as a mere manifestation in the physical space of the second attractor mentioned above, i.e. the rotating mode (or traveling wave). The *apparently solid filaments*, formed by the spontaneous self-assembly of tracer particles, emerge only if the Marangoni number is in a proper range and some specific conditions are satisfied⁵⁻¹¹. In particular, Schwabe and coworkers provided some evidence^{12,13} supporting the idea that PAS may occur *as a resonance between the azimuthally traveling wave and the “turnover time” of the PAS-string in the thermocapillary vortex*.

Most recently, some numerical studies and related possible theories for explaining the ordering of inertial tracers that results in formation of one-dimensional particulate coherent patterns have appeared.

After some initial interesting arguments based on the distinction between fluid and particle inertia^{14,15}, a first concrete step in this direction was undertaken by Melnikov et al.¹⁶.

Theoretical models are under development in which an attempt is being made to explain such dynamics in terms of a “phase locking” process between the hydrothermal traveling wave and the typical frequency of motion of a generic particle (a seminal work along this line of inquiry being represented by Pushkin et al.¹⁷). In such a context, it is also worth mentioning Kuhlmann and Muldoon¹⁸, who addressed the role of “free-surface collisions” in supporting/accelerating the process of transfer of particles from the bulk of liquid to the one-dimensional attracting path.

In the present work the phenomenon is investigated resorting to direct numerical solution (DNS) of the Navier-Stokes equations (together with the energy equation and appropriate boundary conditions) coupled with solution of the Maxey-Riley equation in its simplest form (the so-called “inertial equation” derived by Haller and Sapsis¹⁹ as an explicit dissipative equation describing the flow on the slow manifold that governs the asymptotic behavior of inertial particles). The added value with respect to Pushkin et al.¹⁷ lies in the use of “injected” vorticity to allow a variation of the particle characteristic turnover motion at a fixed (supercritical) value of the Marangoni number (to see how this “added” vorticity interferes

with the oscillatory instability of Marangoni convection and the fundamental mechanism supporting PAS formation).

Starting from the aforementioned cardinal concept of “phase locking”, a more spatial perspective, an application of what is generally regarded as “vorticity thinking”, is invoked and used to elaborate a specific mathematical formalism and some associated important microphysical reasoning. Moreover, this study is extended to the “classical” annular geometry which so much success has enjoyed in the literature for fundamental studies of Marangoni flow and related hierarchy of bifurcations (see, e.g., Li et al.²⁰).

II. MATHEMATICAL MODEL AND METHOD OF ANALYSIS

Both considered geometries (Fig. 1) are featured by a free surface (cylindrical in the liquid-bridge case, planar in the annular-pool case) supporting the development of oscillatory Marangoni convection in the presence of suitable temperature gradients.

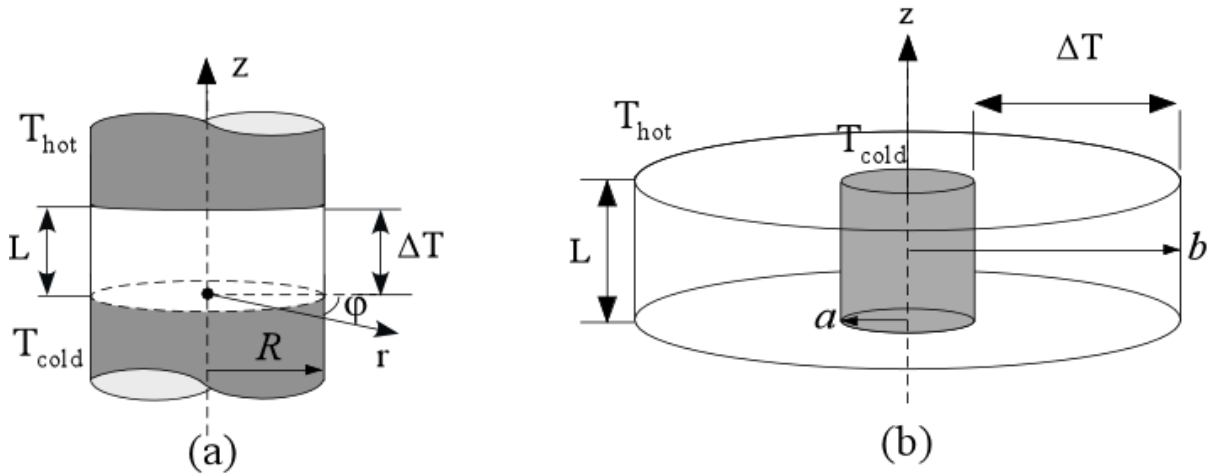


Fig. 1: a) the *liquid bridge*, a drop of liquid with cylindrical free liquid/gas interface held between two differentially heated disks of diameter $D=2R$ placed L apart; b) the *annular pool*, a region having cylindrical symmetry with an open top free surface, a solid bottom, an inner solid wall (radius a), an outer wall (radius b), and depth L .

Furthermore, from a theoretical standpoint, both allow modification of axial vorticity initially existing in the field (associated with the azimuthally traveling hydrothermal wave, which of supercritical Marangoni flow represents the typical manifestation) by imposing a physical rotation of one of the system walls, the top disk in the liquid bridge case or the outer cylindrical wall for the annular configuration (the related Reynolds number is defined here as $Re_{wall}=\Omega_{wall}L^2/\nu$ where L is the system axial extension, Ω_{wall} the imposed angular velocity and ν the fluid kinematic viscosity).

The Navier-Stokes and energy equations have been solved in the nondimensional form obtained by scaling the cylindrical co-ordinates (\bar{r}, \bar{z}) by L and the velocity components in the axial, radial and azimuthal directions $(\bar{V}_z, \bar{V}_r, \bar{V}_\phi)$ by the energy diffusion velocity $V_\alpha = \alpha/L$ [the scales for time (t), pressure (p) and temperature (T) being, respectively, L^2/α , $\rho\alpha^2/L^2$ and ΔT]. These equations read:

$$\underline{\nabla} \cdot \underline{V} = 0 \quad (1)$$

$$\frac{\partial \underline{V}}{\partial t} = -\underline{\nabla} p - \underline{\nabla} \cdot [\underline{V}\underline{V}] + \text{Pr} \nabla^2 \underline{V} \quad (2)$$

$$\frac{\partial T}{\partial t} + \underline{\nabla} \cdot [\underline{V}T] = \nabla^2 T \quad (3)$$

Following the same successful approach of Pushkin et al.¹⁷ the aforementioned inertial equation has been used to track particle motion (such equation allows significant computational simplicity while retaining the fundamental “physics” of the considered class of phenomena). In the frame of reference rotating with the wave the nondimensional form of this equation can be written in compact form as:

$$\underline{V}_{part} = \underline{V} - \eta \frac{D\underline{V}}{Dt} + O(St^2) \quad (4)$$

where \underline{V}_{part} is the particle velocity, \underline{V} is the fluid velocity, $\eta = \frac{\tau\alpha}{L^2}(\xi - 1)$, ξ is the ratio of the particle to the fluid density, τ is the so-called relaxation time, related to the tracer radius \tilde{R} by

the expression $\tau = \frac{2}{9} \frac{\tilde{R}^2}{\nu}$, and the Stokes number St is defined as $St = \frac{2}{9} \left(\frac{\tilde{R}}{L}\right)^2 \frac{UL}{\nu}$, U being

the characteristic flow speed (here we limit to microgravity conditions, hence, buoyancy effects are absent).

The use of this equation implies that, as in the earlier work by Pushkin et al.¹⁷, here PAS structures emerge *only if* η exceeds a threshold value (in other words, only if the particles satisfy given requirements in terms of density and size, as confirmed by experiments; see, e.g., Schwabe et al.¹²). Among other things, this means that all the values of η given in the present manuscript should be seen as values close to (slightly larger than) “threshold values”.

Equations (1-3) have been solved numerically in primitive variables by a time-explicit finite-difference method^{1, 21-22}. The present code was successfully used for numerous studies of Marangoni flows and repeatedly validated also by comparison with other kinds of convection (of various natures, see, e.g., Lappa²).

The flow field required at an arbitrary point of the volume (occupied by the generic moving tracer) for integration of eq. (4) has been linearly interpolated on the computational grid.

Unlike earlier studies [17, 18], where the particle equation was solved “separately” (the 3D solution was frozen to save computational time and the particle tracking equation solved using such a frozen solution as a “background” state), here eq. (4) has been dynamically integrated together with equation (1-3) (i.e. at the same time and with the same time integration step). Moreover, the following strategy has been used to guarantee that the emerging PAS are “physical” (i.e. not numerical artifacts): assuming no particle inertia ($\eta=0 \rightarrow$ no physical PAS of inertial nature can exist), it has been verified that the simulations performed with the time integration step $\Delta t \cong 5 \times 10^{-8}$ (required for the stability of the numerical algorithm used for the solution of the 3D Navier-Stokes equations) did not produce PAS even by prolonging the simulation to $t=50 \times \tau_{PAS}$ where τ_{PAS} is the time for PAS formation when η is in the right range.

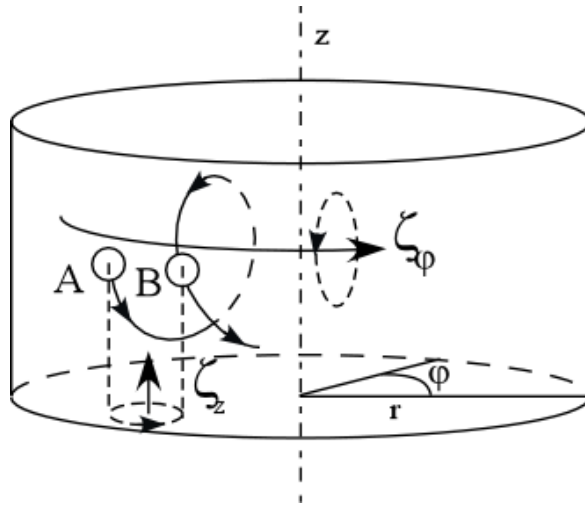


Figure 2: Two consecutive positions taken by a generic particle along its spiral trajectory. The axial and azimuthal components of the associated vorticity vector are also shown.

Let us recall that in Pushkin et al.¹⁷ the model for phase locking was based on the idea that, as originally argued by Schwabe et al.¹², the turnover particle motion, defined as the time needed by a particle in the PAS to perform a complete revolution around the vortex centre (i.e. to move from position A to position B in Fig. 2), may tend to become synchronized with the rotating wave oscillations. In particular, a necessary condition for the existence of PAS was formalized as:

$$\omega_{part} = \omega_{wave} \tag{5}$$

i.e. as the equality between the angular frequencies of the two involved phenomena.

Here we focus expressly on such a relationship.

In such a context, it is convenient to introduce a “spatial way” of thinking, by which the supercritical rotating state of Marangoni flow can be imagined⁵⁻¹³ as the superposition of an axisymmetric toroidal vortex roll (like that existing prior to the onset of 3D flow) and a wave traveling in the azimuthal direction. The two components of vorticity $\underline{\zeta} = \underline{\nabla} \wedge \underline{V}$ in the azimuthal, and axial directions can be written, respectively, as:

$$\zeta_{\varphi} = \left(\frac{\partial V_r}{\partial z} - \frac{\partial V_z}{\partial r} \right) \quad (6a)$$

$$\zeta_z = \frac{1}{r} \left[\frac{\partial}{\partial r} (rV_{\varphi}) - \frac{\partial V_r}{\partial \varphi} \right] \quad (6b)$$

The former contribution is generally regarded as a measure of the strength of the basic Marangoni toroidal flow (Fig. 2). It is, however, the latter contribution that assumes a particularly meaningful role in the present context. Indeed, it is zero in the axisymmetric (steady) state and nonzero in the supercritical state where, more specifically, its half ($\zeta_z/2$) can be regarded as *a measure of the local average angular velocity (spin) of the considered fluid element about the vertical direction*²³. It is hence, on this flow quantity that we concentrate; hereafter for simplicity it will be referred to as Θ_{fluid} or simply Θ (in Fig. 2, for instance, the average value $(\Theta^A + \Theta^B)/2$ would correspond to the average angular spin experienced by a particle moving from A to B).

There is also another important physical connection which allows one to disregard the role played by the other components of vorticity. It is the almost two-dimensional nature of the hydrothermal traveling wave (the wave properties depend significantly on the radial and azimuthal coordinates, but, unless very special conditions are established⁴, the component propagating along the axial direction is rather weak, see, e.g, the review of literature in^{2,4}). This means that an almost perfect analogy can be established between the behavior of the wave in each cross section $z=\text{const}$ and a hypothetical two-dimensional flow with its associated vorticity vector perpendicular to the plane of the flow.

III. RESULTS

Starting point of our analysis is represented by the liquid bridge considered by Melnikov et al.¹⁶ with aspect ratio (height/diameter) $A=0.34$, $Pr=v/\alpha=8$ (NaNO_3), $Ma=20600$ (Marangoni number defined as $\sigma_T \Delta T L / \mu \alpha$ where ΔT is the applied temperature gradient, μ the dynamic viscosity and σ_T the surface tension derivative). Concerning the annular pool, we consider 0.65 cs silicone oil ($Pr=6.7$) and internal and external radii ($a=20$ mm and $b=40$ mm)^{24,25}. The height, is fixed to 20 mm (aspect ratio $A=(b-a)/d=1$). The considered value of the Marangoni number is $Ma=20100$, which corresponds approximately to two times the critical value (Grid $N_z \times N_r \times N_\phi$: $32 \times 40 \times 40$ for the liquid bridge, $36 \times 36 \times 40$ for the annular pool).

PAS structures which form on the traveling wave state of both the liquid bridge and the annular pool (see Figure 3), starting from N particles ($N=4 \times 10^3$) arbitrarily seeded into the field (initially all at rest and contained in two perpendicular meridian planes) are shown as black lines in Figs. 4 and 5.

It is, however, the tracer particles locations representation in space combined with *the isosurfaces of $1/2$ of the axial component of vorticity (Θ_{fluid})* which provides the most interesting insights into the phenomenon.

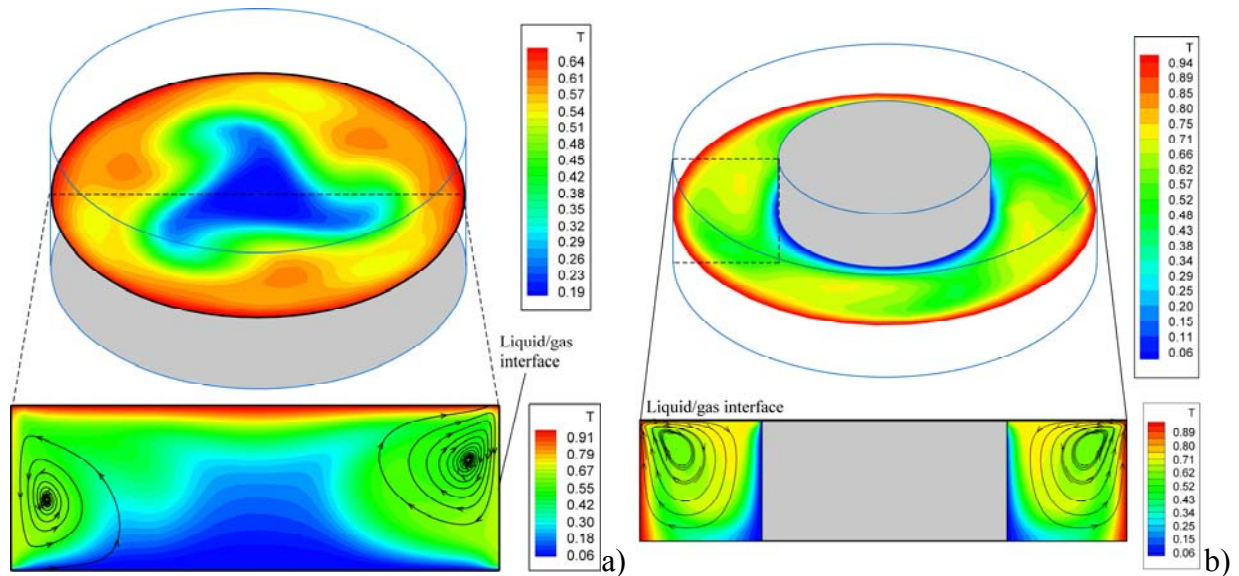


Figure 3: Snapshot of traveling wave state: a) liquid bridge ($Pr=8$, $A=L/D=0.34$, $Ma=20600$, $m=3$, $\omega_{\text{wave}}=71.4$, $Re_{\text{wall}}=0$), b) annular pool ($Pr=6.7$, $A=(b-a)/L=1$, $Ma=20100$, $m=4$, $\omega_{\text{wave}}=38.01$, $Re_{\text{wall}}=0$).

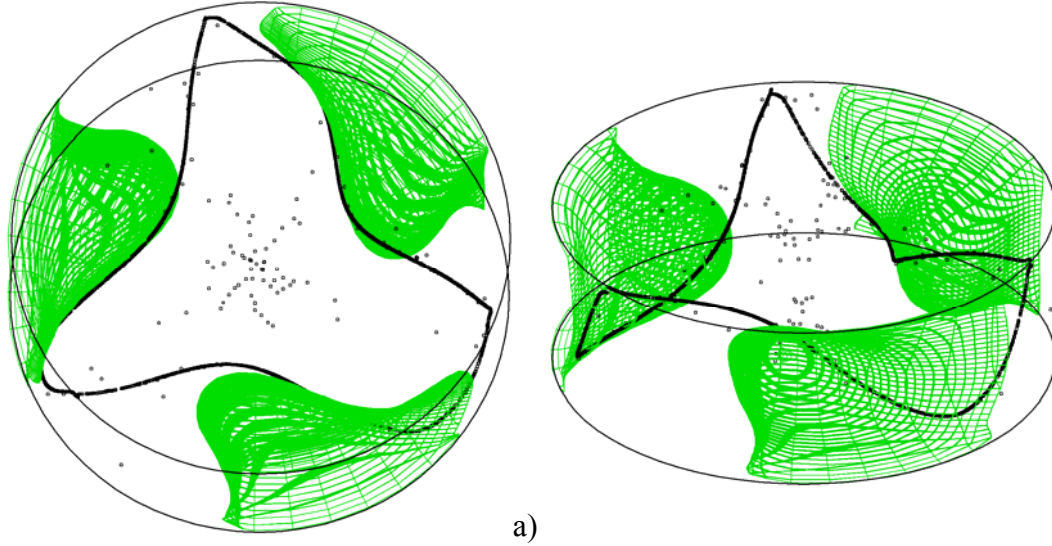


Fig. 4 (color online): Two different views of PAS together with isosurfaces of fluid angular spin plotted for $\Theta_{\text{fluid}}=72$ (liquid bridge, $\text{Pr}=8$, $A=L/D=0.34$, $\text{Ma}=20600$, $m=3$, $\omega_{\text{wave}}=71.4$, $\text{Re}_{\text{wall}}=0$, hot disk on the top, cold disk on the bottom, adiabatic free interface; $\eta=1 \times 10^{-5}$, which corresponds to particles with size $45 \mu\text{m}$ considered by Melnikov et al.¹⁶).

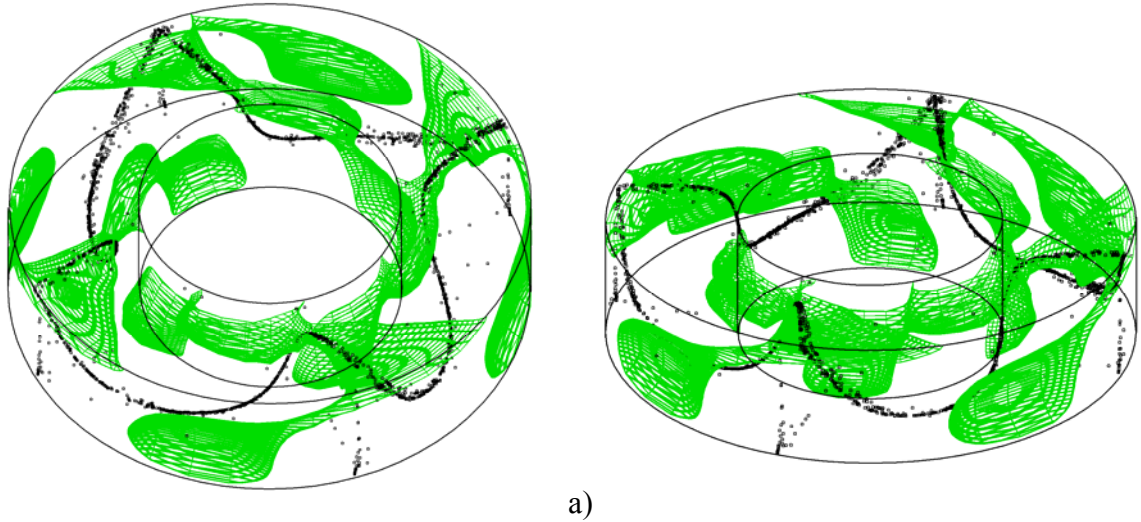


Fig. 5 (color online): Two different views of PAS together with isosurfaces of fluid angular spin plotted for $\Theta_{\text{fluid}}=38$ (annular pool, $\text{Pr}=6.7$, $A=(b-a)/L=1$, adiabatic horizontal boundaries, $\text{Ma}=20100$, $m=4$, $\omega_{\text{wave}}=38.01$, $\text{Re}_{\text{wall}}=0$, $\eta=1 \times 10^{-5}$).

Inspection of Figs. 4 and 5, in fact, reveals that a precise relationship between the one-dimensional closed lines and the two-dimensional isosurfaces of $\Theta_{\text{fluid}}=\zeta_z/2$ can be identified. Indeed, these figures provide evidence that PAS tend to “stay attached” for most of their azimuthal extension to the isosurfaces of fluid axial angular velocity $\Theta_{\text{fluid}} (= \zeta_z/2)$ such that

$$\Theta_{\text{fluid}} = \omega_{\text{wave}} \quad (7)$$

(where ω_{wave} is the angular frequency of the traveling hydrothermal wave defined as $2\pi f/m$, f being the frequency of the temperature oscillation measured at a generic point).

What is even more remarkable in Figs. 4 and 5, is that the spatial shape and curvature of the isosurfaces does not determine solely the one-dimensional pattern created by the projection of the PAS circuit in the xy plane (Figs.4a and 5a); but it also drives the local inclination (with respect to the z axis or equivalently with respect to the horizontal boundaries) of PAS in the 3D space (see, in particular, Figs 4b and 5b).

Equation (7) may be hence regarded as a “practical implementation” of the necessary condition indicated by Pushkin et al.¹⁷ (with Θ_{fluid} representing the asymptotic value of the angular frequency of the turnover particle motion in the limit as the convergence of PAS formation process is attained).

Further elaboration of these key arguments may be provided by referring again to Fig. 2 and using some of the considerations originally reported by Pushkin et al.¹⁷.

As already discussed, it is evident that the vorticity vector associated with the particle spiral motion along the Marangoni toroidal roll has two main components, one directed in the azimuthal direction (corresponding to the motion of the particle in the (r, z) plane) and the other directed axially (corresponding to the displacement undergone by the particle in the (r, φ) plane).

According to Pushkin et al.¹⁷, “*The physical essence of the mechanism lies in the adjustment of the azimuthal particle displacement after every particle turnover due to the inertial interaction with the wave*” (leading to a *modification of the particle azimuthal drift*).

The present numerical simulations corroborate this view by showing that a precise relationships exists for a PAS between the wave frequency and the axial vorticity, where the latter, at this stage, should be seen merely as a “measure” or a proper quantification of *the rate at which the particle local azimuthal displacement takes place*.

IV. DISCUSSION

Under a more general perspective, the empirical observation of the strong geometrical correspondence between the PAS structure and the isosurface of $\frac{1}{2}$ axial vorticity may be seen as the “effect” (we may say a clear manifestation) of the phase locking mechanism, with the phase locking mechanism per se being the “cause”.

Towards the end of further assessing the validity of the above statement, we have considered the possible influence of vorticity artificially injected in the system on the overall PAS formation mechanism. The angular frequency of the traveling wave, in fact, depends on the considered value of the rotation Reynolds number [e.g., for the liquid bridge, $\omega_{\text{wave}} = 71.4, 106.26, 153.92, 230.88, 340.77, 0$ (no inst.) for $\text{Re}_{\text{wall}} = 0, 8.3, 50, 70, 100$ and 200,

respectively; for the annular pool, $\omega_{\text{wave}} = 38.01, 77.21, 0$ (no inst.) for $Re_{\text{wall}} = 0, 30$ and 50 , respectively]. It is evident how the angular frequency becomes higher as Re_{wall} is increased from zero, this trend being limited from above (at high values of Re_{wall}) by the suppression of the Marangoni flow instability^{23, 26}.

Remarkably, we found the value of the η parameter for obtaining convergence of the particle accumulation phenomenon to scale with the Reynolds number as $\cong \eta_0/\sqrt{Re_{\text{wall}}}$ (where η_0 is the value required for $Re_{\text{wall}}=0$), which *from a physical point of view would correspond to particle tracers of decreasing size and/or decreasing density ratio as Re_{wall} is increased*.

Moreover, for Re_{wall} exceeding a given value (depending on the case considered: $Re_{\text{wall}} \cong 30$ and $Re_{\text{wall}} \cong 10$ for the liquid bridge and the annular pool, respectively), some interesting morphological and/or topological changes in the structure of the resulting PAS structures can be observed. These are the emergence of “cusp points” in the projection of the PAS circuit in the xy plane and the displacement toward the top disk of the PAS spatial maxima (points with highest possible values of z) for the liquid bridge (compare Figs. 6a-b); similarly, morphological changes of the PAS branches can be seen for the annular pool when significant wall rotation is applied (the branches are shifted towards the external wall, see Fig. 7a-b).

Paralleling such visible modifications is the increase of the proportionality factor between Θ_{fluid} and ω_{wave} , as witnessed by the plot shown in Figure 8 (where the PAS line clearly stays attached to the isosurfaces of Θ_{fluid} such that $\Theta_{\text{fluid}} = 2\omega_{\text{wave}}$). By contrast, imposed rotation does not seem to have a significant influence on the relationship between the PAS formation time (τ_{PAS}) and the overall hydrothermal wave revolution period, which for all cases has been found to be approximately $\tau_{\text{PAS}} \cong 2 \times \tau_{\text{wave}}$ (where $\tau_{\text{wave}} = 2\pi/\omega_{\text{wave}}$).

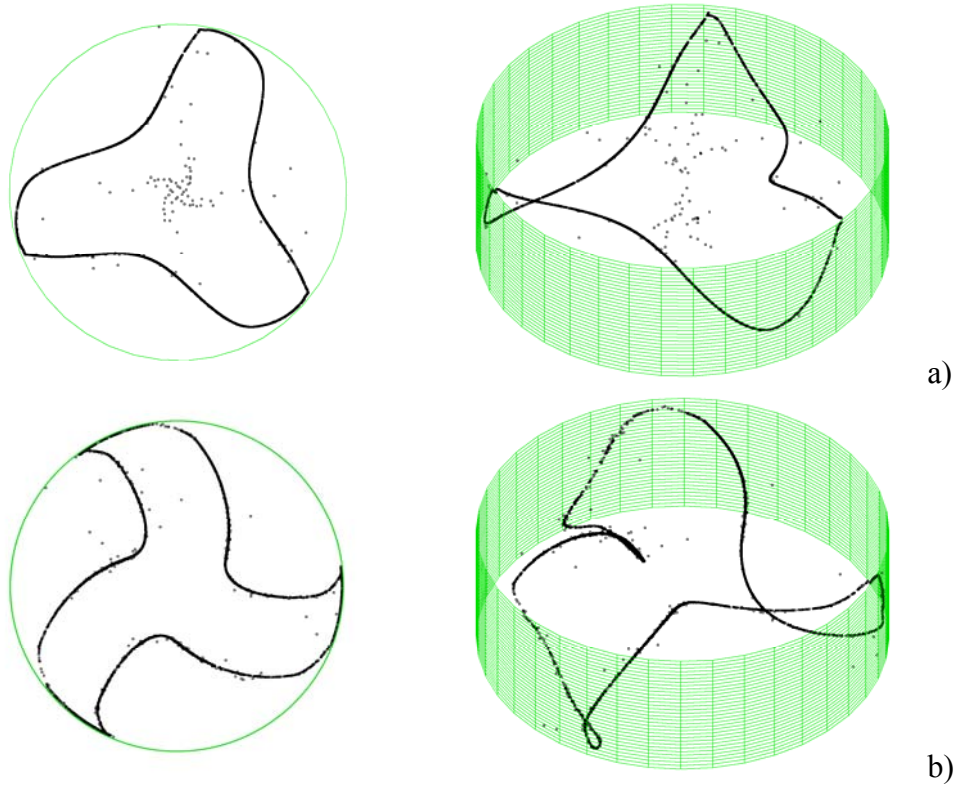


Fig. 6 (color online): Projection of the PAS structure in the xy plane and related 3D view at different values of the rotation Reynolds number for the liquid bridge ($Pr=8$, $A=L/D=0.34$, $Ma=20600$): a) $Re_{wall}=0$; b) $Re_{wall}=50$.

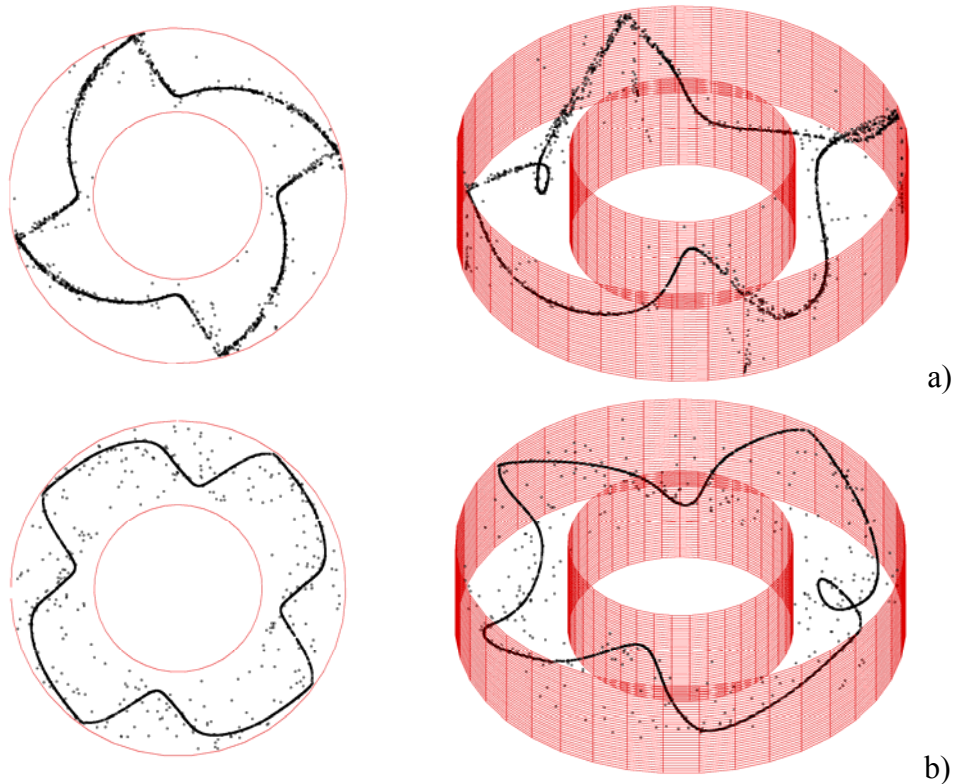


Fig. 7 (color online): Projection of the PAS structure in the xy plane and related 3D view at different values of the rotation Reynolds number for the annular pool ($Pr=6.7$, $A=(b-a)/L=1$, $Ma=20100$): a) $Re_{wall}=0$; b) $Re_{wall}=30$.

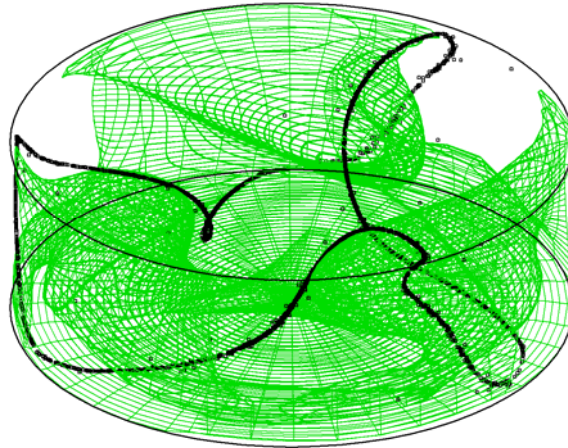


Fig. 8 (color online): Combined view of PAS and isosurfaces of fluid angular spin plotted for $\Theta_{\text{fluid}}=308$ (liquid bridge, $\text{Pr}=8$, $A=0.34$, $\text{Ma}=20600$, $\text{Re}_{\text{wall}}=50$, $m=3$, $\omega_{\text{wave}}=153.92$; z axis direction reversed, rotating hot disk on the bottom, cold disk on the top).

Some additional insights into the influence exerted by imposed rotation on the resulting PAS and related underlying dynamics have been obtained by plotting the trajectory in the laboratory (fixed) frame of a generic particle (pertaining to the PAS structure).

The results for the liquid bridge case are shown in Fig. 9. For $\text{Re}_{\text{wall}}=0$ (Fig. 9a), in particular, one recovers the already known behavior⁶⁻¹³ with the particle moving along a spiral-like string (line) which is wound several times around the Marangoni toroidal roll.

Moreover, the following statements are valid:

- Even if all particle pertaining to the PAS move collectively *such that an illusion of a solid circuit*, rotating at the same angular velocity of the hydrothermal wave, *is created*, such a property, however, only applies to the pattern as such and not to individual particles.
- The particle moves in the azimuthal direction at a velocity relatively small with respect to the angular frequency of the traveling hydrothermal wave, as witnessed by the high number of revolutions (orbits) performed by the particle around the toroidal Marangoni roll to cover 360° (the particle spends much of its time in radial or axial motion, while the rate at which displacement in the azimuthal direction occurs is relatively small, Fig. 9a).

When rotation of the disk is applied (Fig. 9b), the particle follows in space relatively large orbits more extended in the azimuthal and radial directions with respect to the case of no rotation imposed; the projection of such orbits in the xy plane gives approximately circular paths of radius slightly smaller (25% less for $\text{Re}_{\text{wall}}=50$) than the radius of the liquid bridge.

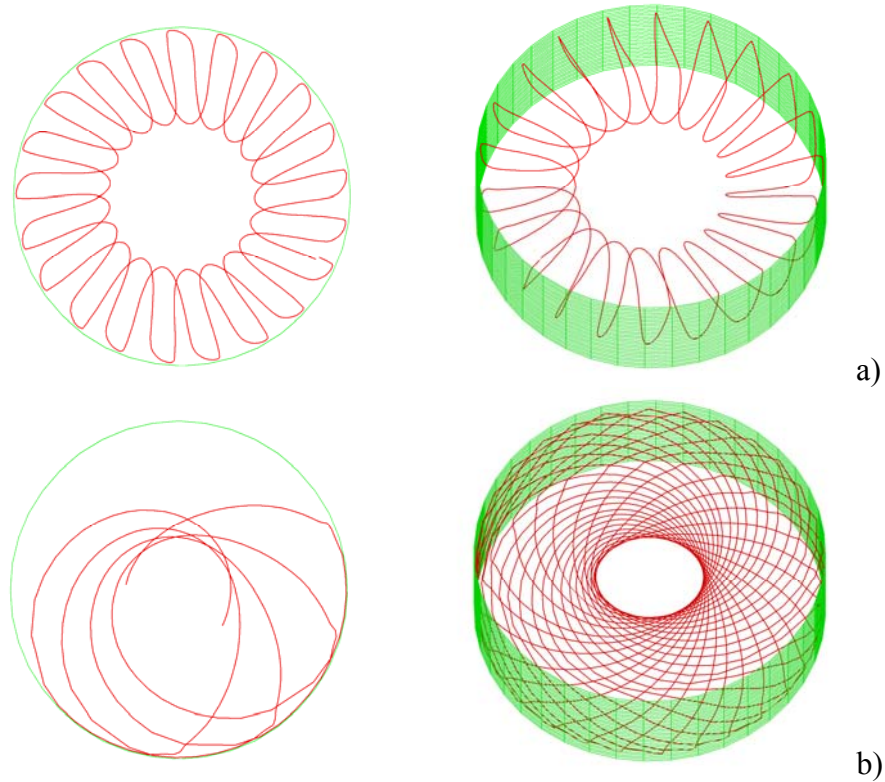


Fig. 9 (color online): Trajectory in the laboratory frame of a generic particle pertaining to the PAS structure (projection in the xy plane and related 3D view) at two distinct values of the rotation Reynolds number for the liquid bridge ($Pr=8$, $A=0.34$, $Ma=20600$): a) $Re_{wall}=0$; b) $Re_{wall}=50$ (the trajectory of the particle and related orbits are plotted for a period corresponding to the overall time required by the particle to come back to its initial azimuthal position, with the exception of the projection of the trajectory in the xy plane for $Re_{wall}=50$, for which only a reduced number of orbits has been included for the sake of clarity).

The increased horizontal extension of such orbits (and the larger time potentially required by the particle to cover each orbit) becomes particularly meaningful in the present context if one considers that it might explain the reason why, *on average*, in the presence of wall rotation, a larger value of the particle angular velocity (a higher integer value of the proportionality factor between Θ_{fluid} and ω_{wave}) is needed to allow phase locking with the traveling wave.

V. CONCLUSIONS

A validation of the so-called “resonant condition” for “phase locking” identified in earlier important works¹⁷ has been developed replacing theoretical entities appearing in the original formulations of such a condition with effective eulerian fluid-dynamic quantities as provided by the numerical simulations. In particular, the basic ideas of the so-called inertial theory for explaining PAS have been illustrated and extended phenomenologically (via numerical simulation) by incorporating ideas of vorticity-wave interactions. More specifically, it has

been shown how the system/problem becomes at once more manageable and more intuitive if it is cast in the form of axial vorticity dynamics and related physical connections with the mechanism supporting the formation of PAS.

Further assessment of the elaborated arguments has been obtained by injecting axial vorticity into the system via rotation of one of its walls. The morphological and spatial properties of PAS change in response to the applied imposed rotation in agreement with the proposed theory/generalization by which PAS form on surfaces where $\frac{1}{2}$ of the axial component of vorticity ζ_z matches the angular frequency of the azimuthally traveling wave produced by the instability of Marangoni flow, or a multiple (integer) of such a frequency.

In particular, a multi-fold effect related to the increase of the rotation Reynolds number has been identified, which is in line with the theoretical arguments developed in this work: First, it increases the characteristic angular frequency of the disturbance traveling in the azimuthal direction; second, the related value of the η parameter for PAS formation scales as $\eta_0/\sqrt{\text{Re}_{\text{wall}}}$, this result being in agreement with the general requirement of inertial theory that the stronger the azimuthal flow (running wave), the smaller the inertia of the particles required in order to determine phase locking with the wave; third, it causes (if Re_{wall} is larger than a give value depending on the case considered) the displacement of the locus of points in space where the condition for phase locking is satisfied towards the rotating boundary (where higher values of Θ_{fluid} occur, axial vorticity being dynamically produced by wall rotation); fourth, the proportionality factor n (integer) between Θ_{fluid} and ω_{wave} increases.

This last effect ($n>1$) might be explained by the influence of imposed rotation on the orbits (revolution motion around the basic Marangoni toroidal roll) which form the trajectory of a generic PAS particle in the fixed (laboratory) frame. Such orbits for $\text{Re}_{\text{wall}}\neq 0$ change their inclination in space from a nearly meridional orientation (in the case of no rotation imposed), to a much more equatorial configuration, this change in inclination being accompanied by a significant increase in the horizontal extension of the orbit (and, therefore, by an increase of the overall distance covered by the particle per orbit, which, in principle, may explain why larger values of the particle azimuthal velocity and Θ_{fluid} are required on average to attain phase locking).

ACKNOWLEDGMENTS

This work is supported by the Italian Space Agency (ASI) in the framework of the JEREMI (Japanese and European Research Experiment on Marangoni Instabilities) Project for the preparation and execution of an experiment onboard the International Space Station (ISS).

REFERENCES

- [1] M. Lappa, *Fluids, Materials and Microgravity: Numerical Techniques and Insights into the Physics*, (Elsevier Science, Oxford, England, 2004).
- [2] M. Lappa, *Thermal Convection: Patterns, Evolution and Stability* (John Wiley & Sons, Chichester, England, 2010); M. Lappa, Thermal convection and related instabilities in models of crystal growth from the melt on earth and in microgravity: Past history and current status, *Cryst. Res. Technol.*, **40**(6), 531 (2005).
- [3] M. Lappa, Some considerations about the symmetry and evolution of chaotic Rayleigh–Bénard convection: The flywheel mechanism and the “wind” of turbulence, *C. R. Méc.*, **339**, 563 (2011).
- [4] V. Shevtsova, D.E. Melnikov, A. Nepomnyashchy, New flow regimes generated by mode coupling in buoyant-thermocapillary convection, *Phys. Rev. Lett*, **102**, 134503 (2009).
- [5] D. Schwabe, P. Hintz, S. Frank, New Features of Thermocapillary Convection in Floating Zones Revealed by Tracer Particle Accumulation Structures, *MST*, **9**, 163 (1996).
- [6] I. Ueno, S. Tanaka and H. Kawamura, Oscillatory and chaotic thermocapillary convection in a half-zone liquid bridge, *Phys. Fluids*, **15**(2), 408 (2003).
- [7] I Ueno, S. Tanaka and H. Kawamura, Various flow patterns in thermocapillary convection in half-zone liquid bridge of high prandtl number fluid, *Adv. Space Res.*, **32**(2), 143 (2003).
- [8] D. Schwabe, A. I. Mizev, S. Tanaka and H. Kawamura, Particle accumulation structures in time-dependent thermocapillary flow in a liquid bridge under microgravity, *Microgravity Sci. Tech.*, 18(3-4), **117** (2006).
- [9] S. Tanaka, H. Kawamura, I. Ueno, D. Schwabe, Flow structure and dynamic particle accumulation in thermocapillary convection in a liquid bridge, *Phys. Fluids*, **18**, 067103 (2006).
- [10] Y. Abe, I. Ueno and H. Kawamura, Effect of shape of HZ liquid bridge on particle accumulation structure (PAS), *Microgravity Sci. Tech.*, **19**(3-4), 84 (2007).
- [11] I. Ueno, Y. Abe, K. Noguchi, and H. Kawamura, Dynamic particle accumulation structure (PAS) in half-zone liquid bridge - Reconstruction of particle motion by 3-D PTV, *Adv. Space Res.*, **41**(12), 2145 (2008).
- [12] D. Schwabe, A.I. Mizev, M. Udhayasankar and S. Tanaka, Formation of dynamic particle accumulation structures in oscillatory thermocapillary flow in liquid bridges, *Phys. Fluids*, **19**(7), 072102 (2007).

- [13] D. Schwabe and A.I. Mizev, Particles of different density in thermocapillary liquid bridges under the action of travelling and standing hydrothermal waves, *Eur. Phys. J. Special Topics* **192**, 13 (2011).
- [14] D. V. Lyubimov, T. P. Lyubimova and A. V. Straube, Accumulation of solid particles in convective flows, *Microgravity Science and Technology*, **16**(1-4), 210 (2005).
- [15] S. Domesi, Particle dynamics in the axisymmetric toroidal flow in thermocapillary liquid bridges: towards understanding PAS, *Sci. Tech.*, **18** (3-4), 137 (2006).
- [16] D. Melnikov, D. Pushkin, and V. Shevtsova, Accumulation of particles in time-dependent thermocapillary flow in a liquid bridge. Modeling of experiments, *Eur. Phys. J. Special Topics*, **192**, 29 (2011).
- [17] D. Pushkin, D. Melnikov, V. Shevtsova, Ordering of Small Particles in One-Dimensional Coherent Structures by Time-Periodic Flows, *Phys. Rev. Lett.*, **106**, 234501 (2011).
- [18] H.C. Kuhlmann and F.H. Muldoon, Particle-accumulation structures in periodic free-surface flows: Inertia versus surface collisions, *Phys Rev. E*, **85**, 046310 (2012) [5 pages].
- [19] G. Haller and T. Sapsis, Where do inertial particles go in fluid flows?, *Physica D: Nonlinear Phenomena*, **237**(5), 573 (2008).
- [20] Y.R. Li, L. Peng, W.Y. Shi and N. Imaishi, Convective instabilities in annular pools, *Fluid Dyn. Mater. Process.*, **2**(3), 153 (2006).
- [21] M. Lappa and R. Savino, Parallel solution of the three-dimensional Marangoni flow instabilities in liquid bridges, *Int. J. Num. Meth. Fluids*, **31**, 911 (1999); M. Lappa, R. Savino, 3D analysis of crystal/melt interface shape and Marangoni flow instability in solidifying liquid bridges, *Journal of Computational Physics*, **180** (2), 751 (2002).
- [22] M. Lappa, Three-dimensional numerical simulation of Marangoni flow instabilities in floating zones laterally heated by an equatorial ring, *Phys. Fluids*, **15**(3), 776 (2003); Combined effect of volume and gravity on the three-dimensional flow instability in non-cylindrical floating zones heated by an equatorial ring, *Phys. Fluids*, **16**(2), 331 (2004).
- [23] M. Lappa *Rotating Thermal Flows in Natural and Industrial Processes* (John Wiley & Sons, Chichester, England, 2012).
- [24] D. Schwabe and S. Benz, Thermocapillary flow instabilities in an annulus under microgravity - Results of the experiment MAGIA, *Adv. Space Res.*, **29**, 629 (2002).
- [25] Y.R. Li, L. Peng, Y. Akiyama and N. Imaishi, Three-dimensional numerical simulation of thermocapillary flow of moderate Prandtl number fluid in an annular pool, *J. Cryst. Growth*, **259**, 374 (2003)

[26] Ch.-H. Chun, and W. Wuest, Suppression of temperature oscillations of thermal Marangoni convection in a floating zone by superimposing of rotating flows, *Acta Astronautica*, **9**(4), 225 (1982).